

## Measurement of the Neutron Lifetime by Counting Trapped Protons

J. Byrne, P. G. Dawber, J. A. Spain, and A. P. Williams<sup>(a)</sup>  
*University of Sussex, Falmer, Brighton BN1 9QH, United Kingdom*

M. S. Dewey, D. M. Gilliam, G. L. Greene, and G. P. Lamaze  
*National Institute of Standards and Technology, Gaithersburg, Maryland 20899*

R. D. Scott

*Scottish Universities Research and Reactor Center, East Kilbride, Glasgow G75 0QU, United Kingdom*

J. Pauwels, R. Eykens, and A. Lamberty

*Commission of the European Communities, Joint Research Center,  
 Central Bureau for Nuclear Measurements, B-2440 Geel, Belgium*

(Received 21 March 1990)

The neutron lifetime  $\tau_n$  has been measured by counting decay protons stored in a Penning trap whose magnetic axis coincided with a neutron-beam axis. The result of the measurement is  $\tau_n = 893.6 \pm 5.3$  s which agrees well with the value predicted by precise measurements of the  $\beta$ -decay asymmetry parameter  $A$  and the standard model.

PACS numbers: 14.20.Dh, 13.30.Ce

Self-consistency among experimental values for the neutron lifetime  $\tau_n$ , the various angular and polarization correlation coefficients in free-neutron  $\beta$  decay, and  $ft$  values of pure Fermi  $0^+ \rightarrow 0^+$  superallowed  $\beta$  transitions provides one of the best tests of the standard  $V-A$  theory of semileptonic weak processes.<sup>1</sup> For neutron decay, the accumulated data are sufficiently accurate to establish useful limits on departures from the standard model.<sup>2</sup> The availability of an accurate value for  $\tau_n$  also has important implications for cosmology<sup>3</sup> and astrophysics.<sup>4</sup>

There are two distinct strategies for the direct determination of  $\tau_n$ . The usual procedure<sup>5</sup> is an "in-beam" method whereby the neutron decay rate  $\dot{N}_n$  is measured in a well-defined volume through which a neutron beam passes. If  $N_n$  is the mean neutron number in that volume,  $\tau_n$  is determined by application of the differential equation  $\dot{N}_n = -N_n/\tau_n$ . This method requires absolute measurements of the event rate, beam volume, and time-averaged neutron density within that volume. In neutron "bottle" experiments<sup>6</sup> an isolated ensemble of  $N(0)$  neutrons is confined for a time  $t$  and  $\tau_n$  is determined by application of the exponential relation  $N(t) = N(0)e^{-t/\tau_n}$ . Such methods have advanced dramatically in recent years; nevertheless, they require very careful assessment of loss mechanisms.

The present experiment is of the in-beam variety where the beam volume is defined by the boundaries of an electromagnetic Penning trap.<sup>7</sup> The trap retains all protons produced by neutron decay in the cold neutron beam which traverses it parallel to the magnetic axis. These protons are subsequently ejected from the trap and counted with near unit efficiency. Simultaneously, the mean neutron density is determined by counting with known efficiency the  $\alpha$  particles from the  $^{10}\text{B}(n, \alpha)^7\text{Li}$  re-

action. In an earlier version of this technique<sup>8</sup> the magnetic field was oriented normal to the neutron beam.

In the parallel configuration any dependence on the spatial distribution and velocity distribution of the neutrons within the neutron beam is eliminated<sup>7</sup> and  $\tau_n$  is given by

$$\tau_n = \left( \frac{N_\alpha}{\epsilon_0} \right) \left( \frac{\epsilon_p}{N_p} \right) \left( \frac{L}{v_0} \right). \quad (1)$$

Here  $N_p$  and  $N_\alpha$  are the numbers of protons and  $\alpha$  particles, respectively, recorded in an arbitrary counting period,  $L$  is the length of the neutron beam which decays in the trap, and  $\epsilon_p$  is the efficiency of the proton detector.  $\epsilon_0 = (\Omega/4\pi)\rho_s\sigma_0 N_A/A$  is the efficiency for counting a thermal neutron of velocity  $v_0 = 2200 \text{ m s}^{-1}$ , where  $\Omega/4\pi$  is the relative solid angle for  $\alpha$ -particle collection,  $\rho_s$  is the surface density in  $\text{g/cm}^2$  of  $^{10}\text{B}$  atoms ( $A = 10.0129$ ),  $\sigma_0$  is the thermal cross section, and  $N_A$  is Avogadro's number.

A schematic of the apparatus used in the experiment is shown in Fig. 1. The Penning trap consists of two potential barriers  $\approx 1$  kV high, superimposed on a coaxial 5-T uniform magnetic field produced by a superconducting solenoid. Trapped protons of energy  $< 0.751$  keV move in cyclotron orbits of radii  $< 1$  mm about the local magnetic field lines. Their guiding centers move along the magnetic field lines between the confining or "mirror" electrode and the "gate" electrode through which the protons are periodically released. Trapping times between 5 and 100 ms were studied to confirm that there was no diffusion loss of trapped protons. Final data were all taken with a 10-ms trapping time.

Because of the presence of energy- and electric-field-dependent end effects, the mean trap length is difficult to

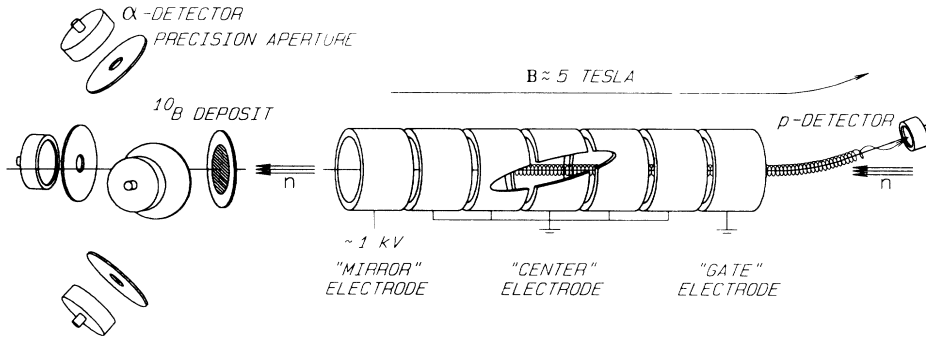


FIG. 1. Schematic outline of the experimental method showing the gate electrode in the trap-open configuration. The actual proton trap has sixteen independent electrode segments.

determine precisely. The trap is therefore constructed from sixteen segments, each of which is fabricated from fused quartz to optical tolerances, coated with a conducting layer, and electrically connected to its own high-voltage switch. Each segment is nominally 22 mm long and its length is known to better than  $\pm 10 \mu\text{m}$ . By employing a range of trap lengths, it is possible to eliminate the end effects entirely and determine the differential decay rate  $dN_p/dL$ , i.e., the number of trapped protons per unit length of beam, which replaces  $N_p/L$  in Eq. (1). An experimental plot of  $N_p$  against  $L$  is shown in Fig. 2 which reveals no deviation from linearity.

To release the trapped protons the "gate" electrode facing the detector is lowered to ground potential, and the protons exit with their guiding centers moving adiabatically along the magnetic field lines. These field lines bend by  $9.5^\circ$  in the region beyond the trap. Besides bending, the magnetic field decreases slightly in this re-

gion to avoid creating a magnetic mirror for low-energy protons. Finally, the protons are accelerated into a silicon-surface-barrier detector, which is held at a high negative potential. The resulting signal is transmitted to ground through an optical fiber. Typical acceleration voltages range between 20 and 40 kV, allowing easy discrimination of protons from counter noise. The back-

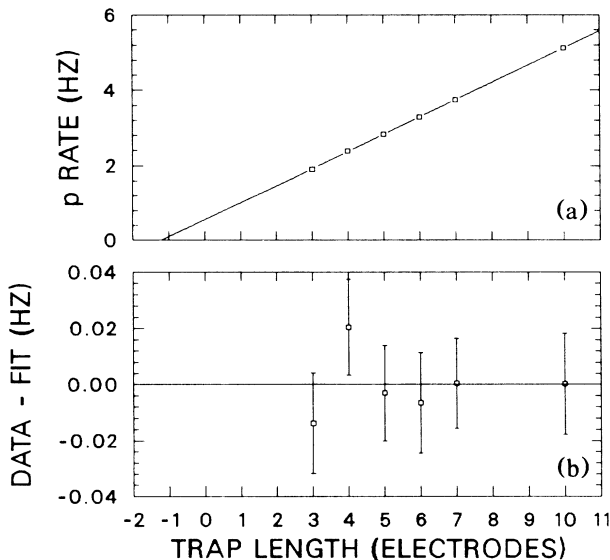


FIG. 2. A plot of (a) proton count rate vs trap length and (b) residuals. The slope of this line is the activity per unit length of the neutron beam.

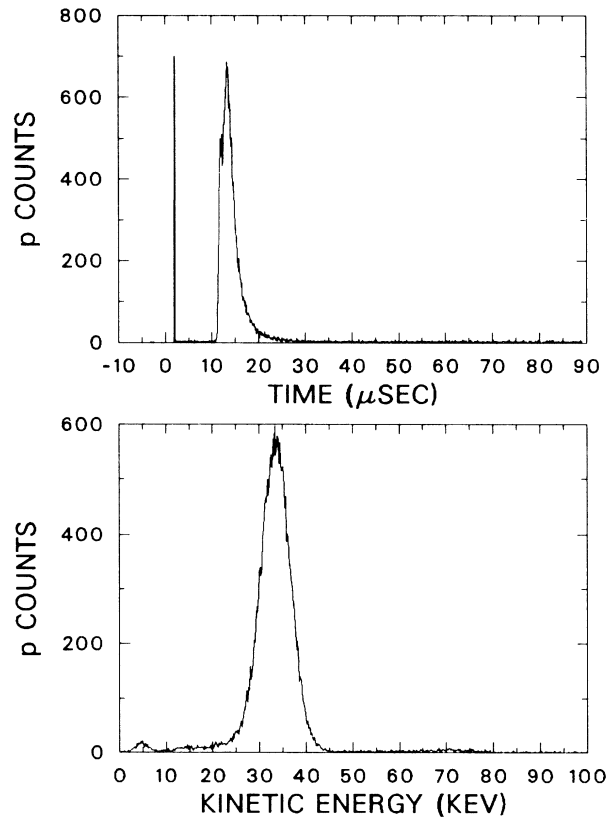


FIG. 3. (a) A histogram of proton counts vs arrival time at the detector. Time  $t=0$  corresponds to the signal which triggers the "opening" of the Penning trap. The sharp peak shortly after  $t=0$  is an artifact. (b) A histogram of proton counts vs energy. The decay signal is seen with very high signal-to-noise ratio.

ground is further suppressed by a factor  $> 100$  by gating the counter only during the appropriate "trap-open" interval.<sup>8</sup> Following proton collection, the "mirror" electrode is grounded for  $10 \mu\text{s}$  to release any trapped decay electrons of energy  $< 1 \text{ keV}$ . This is the source of the electrode timing correction listed in Table II.

The distribution of observed proton events versus energy and time of arrival is shown in Fig. 3 where the signal-to-noise ratio is typically about 500. The timing spectrum was used in the final data analysis because the background and dead-time corrections are more straightforward in this case. A timing-spectrum event signals the arrival of one or more protons in the trap or a background pulse. In the energy spectrum, it is sometimes difficult to distinguish multiproton events from true background.

After traversing the proton trap, the neutron beam passes through a 0.34-mm-thick single crystal of silicon which supports a 94%  $^{10}\text{B}$  enriched deposit. Those  $\alpha$  particles from the reaction  $^{10}\text{B}(n,\alpha)^7\text{Li}$  that are emitted in the backward direction are inhibited by the silicon wafer from reaching the proton trap where they could generate background by ionization. Those emitted in the forward direction suffer negligible scattering or energy loss when emerging from the deposit and are recorded by four surface-barrier detectors. The total collection solid angle  $\Omega$  was determined by four precision apertures. It was measured in two ways: by mechanical contact metrology and by calibration with  $\alpha$  sources of known absolute activity. These methods agreed to within 0.1%, yielding the result  $\Omega/4\pi = 0.004196 \pm 0.1\%$ .

The  $^{10}\text{B}(n,\alpha)^7\text{Li}$  cross section  $\sigma(v)$  is known to deviate from pure  $1/v$  behavior (as reflected by the Westcott  $g$  factor) by  $\lesssim 0.03\%$  (Ref. 9) and has the thermal value  $3839.5 \pm 0.16\% \text{ b}$ .<sup>10</sup> The  $^{10}\text{B}$  surface density  $\rho_s$  was determined on the basis of isotope dilution mass spec-

TABLE I. Results for several detector voltages and gold thicknesses.  $\epsilon_p$  corrects for elastic Rutherford scattering of protons from the detector surface. The quoted errors are the statistical errors on each individual  $dN_p/dL$  determination. The statistically combined result needs to be adjusted for several small effects.

Detector voltage (kV)	Au thickness ( $\mu\text{g}/\text{cm}^2$ )	$\epsilon_p$	$\left(\frac{N_d}{\epsilon_0}\right)\left(\frac{\epsilon_p}{v_0}\right)\left(\frac{dN_p}{dL}\right)^{-1}$ (s)
24.5	38.6	0.9743	$886.0 \pm 11.4$
29.5	18.3	0.9924	$894.3 \pm 5.7$
32.0	18.3	0.9936	$892.7 \pm 4.7$
34.5	18.3	0.9945	$903.1 \pm 8.4$
32.0	58.9	0.9762	$938.0 \pm 21.5$

troscopy on selected samples from a range of  $^{10}\text{B}$  and  $^6\text{LiF}$  deposits, whose counting rates were compared in a neutron beam at the BR1 reactor, Studiecentrum voor Kernenergie, Centre d'Etudes Nucleaires, Mol, Belgium.<sup>11</sup> The result for the  $^{10}\text{B}$  foil (No. 2-H4) which was used in the present experiment was  $\rho_s = 11.934 \pm 0.037 \mu\text{g}/\text{cm}^2$ .

The data used to determine the present result were derived from five complete runs carried out at the cold beam position PN7 at the Institut Laue-Langevin, Grenoble, France. Several different accelerator voltages were used in conjunction with several surface-barrier detectors having a variety of measured gold-window thicknesses. The data are summarized in Table I, together with calculated values of  $\epsilon_p$  which depart slightly from unity because of Rutherford scattering in the gold window or, with less probability, in the silicon substrate. Most of the data were obtained with detectors having  $20 \mu\text{g}/\text{cm}^2$  of gold so that backscattering was minimized.

TABLE II. Final results and corrections.

Correction (s)	Uncertainty (s)	Source of correction
0.0	2.8	Boron foil mass per unit area
0.0	1.4	$^{10}\text{B}$ cross section
0.1	1.0	$n$ detector solid angle for finite $n$ beam
0.0 <sup>a</sup>	1.0	$p$ backscattering from gold surface of detector
2.8	0.7	Absorption of neutrons by boron
0.0 <sup>a</sup>	0.5	$p$ backscattering from silicon in detector
-3.6	0.5	Finite-radius $n$ beam on nonuniform boron deposit
-0.9	0.5	Electrode timing
-0.7	0.5	Incoherent $n$ scattering in silicon backing of $^{10}\text{B}$ deposit
0.0	0.5	Trap length
0.8	0.2	Absorption of neutrons by silicon backing
-1.5	3.7	Total correction for systematic effects
895.1	3.8	Uncorrected statistical result
893.6	5.3	Final $1\sigma$ result

<sup>a</sup>Corrections for these effects were applied to individual runs.

The other detectors were used primarily as a check on the systematic variation of the backscattering. Corrections with uncertainties for important systematic effects are listed in Table II. The largest correction is present because the boron deposit was not uniformly distributed on the foil (there were more target atoms available in the center).<sup>11</sup> This distribution was sampled by a neutron beam roughly 16 mm in diameter at the foil. As it happens, this adjustment is nearly compensated for by one made for absorption of neutrons in the boron foil (there were fewer neutrons deeper in the target). Our final result is  $\tau_n = 893.6 \pm 5.3$  s where the stated error is the quadratic sum of systematic and statistical errors. This result agrees with the recent value of  $887.6 \pm 3$  s obtained by Mampe *et al.*,<sup>6</sup> and with the latest  $g_A/g_V$  value<sup>12</sup> which, when taken with the value of  $g_V$  derived from  $0^+ \rightarrow 0^+$  nuclear  $\beta$  decays,<sup>13</sup> and the phase-space factor,<sup>1</sup> gives  $897.4 \pm 3.7$  s.

We note the discrepancy between our result and the earlier result of Byrne *et al.*<sup>8</sup> We now recognize that incorrect values for the calibration and uniformity of the neutron counting foils were used in the 1980 experiment.<sup>11</sup> Other defects associated with end-effect uncertainties and proton loss by magnetic mirror trapping have been eliminated in the present work as well.

We wish to thank Professor J. M. Robson for his support and interest in this work, Dr. Klaus Schreckenbach for the considerable assistance and technical support provided by him and other members of the staff at the Institut Laue-Langevin, J. Van Gestel for his outstanding contribution in the preparation of the  $^{10}\text{B}$  and  $^6\text{LiF}$  reference deposits, and Dr. Nalin Parikh of the University of North Carolina for the measurements of the gold-window thicknesses. One of us (A.P.W.) also wishes to thank the Institut Laue-Langevin for financial support.

This work was supported in part by DOE interagency agreement No. DE-AI05-87ER40340 and by the Science and Engineering Research Council of the United Kingdom. We also acknowledge a travel grant from NATO.

<sup>(a)</sup>Present address: Institut Laue-Langevin, Grenoble, France.

<sup>1</sup>D. H. Wilkinson, Nucl. Phys. **A377**, 474 (1982).

<sup>2</sup>A. S. Carnoy, J. Deutsch, and B. R. Holstein, Phys. Rev. D **38**, 1636 (1988).

<sup>3</sup>D. N. Schramm and L. Kawano, Nucl. Instrum. Methods Phys. Res., Sect. A **284**, 84 (1989).

<sup>4</sup>J. N. Bahcall *et al.*, Rev. Mod. Phys. **54**, 767 (1982).

<sup>5</sup>C. J. Christensen *et al.*, Phys. Rev. D **5**, 1628 (1972); L. N. Bondarenko *et al.*, Pis'ma Zh. Eksp. Teor. Fiz. **28**, 328 (1978) [JETP Lett. **28**, 303 (1978)]; P. E. Spivak, Zh. Eksp. Teor. Fiz. **94**, 1 (1988) [Sov. Phys. JETP **67**, 1735 (1988)]; J. Last *et al.*, Phys. Rev. Lett. **60**, 995 (1988); K. Schreckenbach *et al.*, Nucl. Instrum. Methods Phys. Res., Sect. A **284**, 120 (1989).

<sup>6</sup>W. Mampe *et al.*, Phys. Rev. Lett. **63**, 593 (1989); V. Morozov, Nucl. Instrum. Methods Phys. Res., Sect. A **284**, 108 (1989); F. Anton *et al.*, Z. Phys. C **45**, 25 (1989).

<sup>7</sup>J. Byrne *et al.*, Nucl. Instrum. Methods Phys. Res., Sect. A **284**, 116 (1989).

<sup>8</sup>J. Byrne *et al.*, Phys. Lett. **92B**, 274 (1980).

<sup>9</sup>B. A. Magurno, R. R. Kinsey, and F. M. Scheffel, *Guidebook for the ENDF/B-V Nuclear Data Files* (BNL Report No. BNL-NCS-31451, 1982).

<sup>10</sup>R. Peele and H. Condé, in *Proceedings of the International Conference on Nuclear Data for Science and Technology, Mito, Japan, 1988*, edited by S. Igarasi (Japan Atomic Energy Research Institute, Tokai-mura, 1988), p. 1005.

<sup>11</sup>J. Pauwels *et al.*, in *Proceedings of the Fifteenth INTDS World Conference, Santa Fe, September 1990* (to be published).

<sup>12</sup>P. Bopp *et al.*, Phys. Rev. Lett. **56**, 919 (1986).

<sup>13</sup>J. C. Hardy *et al.*, Nucl. Phys. **A509**, 429 (1990).